

This paper has been accepted for publication in the  
*Journal of Geophysical Research- Atmospheres*.  
Copyright (2013) American Geophysical Union. Further  
reproduction or electronic distribution is not permitted.

**The potential of commercial microwave networks to monitor dense fog-  
feasibility study**

**N. David<sup>1</sup>, P. Alpert<sup>1,2</sup>, and H. Messer<sup>3</sup>**

<sup>1</sup> The Department of Geophysical, Atmospheric and Planetary Sciences, Tel-Aviv University, Tel Aviv, Israel.

<sup>2</sup> The Porter School of Environmental Studies and the Department of Geophysical, Atmospheric and Planetary Sciences Tel-Aviv University, Tel Aviv, Israel.

<sup>3</sup> The School of Electrical Engineering, Tel-Aviv University, Tel Aviv, Israel

Correspondence to: N. David ([noamda@post.tau.ac.il](mailto:noamda@post.tau.ac.il))

This article has been accepted for publication and undergone full peer review but has not been through the copyediting, typesetting, pagination and proofreading process which may lead to differences between this version and the Version of Record. Please cite this article as doi: 10.1002/2013JD020346

## Abstract

Here we show the potential for dense fog monitoring using existing measurements from wireless communication systems. Communication networks widely deploy commercial microwave links across the terrain at ground level. Operating at frequencies of tens of GHz they are affected by fog and are, practically, an existing, sensor network, spatially distributed world-wide, that can provide crucial information about fog concentration and visibility.

The goal of this paper is to show the feasibility for fog identification and intensity estimation.

A method is proposed and is demonstrated by two cases of heavy fog that took place in Israel.

During these events, fog covered wide areas (tens of kilometers) and caused severe decrease in visibility, dropping as low as several tens of meters. Liquid water content and visibility values were estimated using measurements from tens of microwave links deployed in the

observed area for each event. Each of the links provided a single measurement which was taken simultaneously across all of the links in the system. The values were found to be in the range of  $0.5\text{-}0.8\text{ gr/m}^3$  – high concentration values that match the maximum value range observed in field measurements carried out for prior studies in different test areas in the world. The visibility ranges calculated, between 30 and 70 meters, fit the visibility assessments from the specialized measuring equipment operating in the observed area at the same time. These results point to the strong potential of the proposed technique.

## 1 Introduction

Fog is defined as water droplets suspended in the atmosphere, near the surface of earth that reduce visibility to less than 1 km [AMS, 2000]. The impact of fog on human beings and on the environment is considerable. Fog harvesting, for instance, can produce fresh water for gardening, afforestation and even potable water that may have a significant contribution particularly in water scarce regions [Oliver, 2004; Klemm et al., 2012]. Moreover, in forest ecosystems, fog takes a cardinal part in the water balance of these natural environments [Dawson, 1998; Wrzesinsky and Klemm, 2000]. Information concerning the Liquid Water Content (LWC) of fog makes it possible to define the concentration of air pollutants through analysis of fog droplet samples [Tago et al., 2006]. An important role fog plays in cleaning the atmosphere through the process of particle scavenging and then drop deposition has also been shown [Herckes et al., 2007]. On the other hand, smog (a portmanteau of smoke and fog) may harm human health, adversely affect plants and damage structures [e.g. Wichmann et al., 1989; Dam and Hoang, 2008]. However, the central negative effect attributed to fog, is reduced visibility that can lead to heavy financial damages, grave accidents and loss of life [Croft et al., 1995; Pagowski et al., 2004, Gultepe et al., 2009]. The total economic impact of the presence of fog on aviation, marine and land transportation can reasonably be compared to the impact of tornadoes or, in some cases, even those of hurricanes [Gultepe et al, 2007]. Furthermore, it has been recently shown that while the number of road accidents due to rain has declined considerably, the totals in foggy conditions have not changed significantly [Pisano et al., 2008].

Existing means of measuring fog provide reliable measurements in most cases, but are limited in the spatial range they can cover, in their availability, and by their high implementation costs. Predominant techniques for detection of fog and measuring visibility include: trained human observers, transmissometers, satellites and instruments that measure

the scatter coefficient. A trained human observer assesses visibility by the appearance or occlusion of objects at known distances from the observer's present location. However, this assessment is a subjective judgment by a particular observer, one observer's estimation might disagree with another's when assessing the same visibility conditions. One of the most common instruments for measuring the light extinction coefficient is the transmissometer [WMO, 2008]. Although this device is considered very accurate, its costs are extremely high. An additional technique includes instruments measuring the scatter coefficient of light [WMO, 2008]. However, this technique only allows for a small sample volume to be measured. As a result, the visibility representativeness obtained is poor. Satellites have the advantage of providing large spatial coverage. Nevertheless, in some cases, they struggle to supply fog detections at ground level. High or middle altitude clouds along the line of sight between the ground and the system may obscure ground level fog [e.g. Ellrod, 1995]. It is also difficult to differentiate, using this technique, whether the observation reflects actual fog, or low stratus clouds, found at higher levels off the surface. Some instruments were designed to provide measurements of the fog LWC. While all are spatially limited, commonly used tools include the Particle Volume Monitor (PVM), Forward Scattering Spectrometer Probe (FSSP) and hot-wire probes [Gerber, 1984; Arends et al., 1992; Emert, 2001; Schwarzenboeck et al., 2009].

At frequencies of tens of GHz, various atmospheric hydrometeors: precipitation, water vapor, sleet, mist and fog affect microwave beams, causing perturbations to radio signals [Rec. ITU-R P.838-2, 2004; Rec. ITU-R P.676-6, 2005; Rec. ITU-R P.840-4, 2009]. Thus, wireless communication networks can be considered to be built in environmental monitoring facilities, as was first demonstrated for rainfall observations [Messer et al. 2006; Leijnse et al., 2007a]. In particular, wireless communication networks seem to have suitable properties and the potential to monitor fog with certain potential advantages over existing monitoring tools.

Typically, the Microwave Links (MLs) utilized in these networks are installed at heights of a few tens of meters off the surface, they are widely spread across the terrain and provide continuous measurements at high temporal and spatial resolution. Finally, the implementation costs are minimal since the requested data are standard data collected and logged routinely by the communication providers. However, most of the work done in this field of research till today was focused on the ability to monitor rainfall [e.g. Rayitsfeld et al., 2011; Chwala et al., 2012; Wang et al., 2012]. The ability to reconstruct the rainfall intensity distribution using multiple MLs in a given area has also been described [e.g. Goldshtein et al., 2009; Zinevich et al., 2008,2009]. Only a limited amount of research has investigated the potential for monitoring other-than-rain phenomena using measurements from MLs. These works include for example: estimating the areal evaporation [Leijnse et al.,2007b] and measuring the atmospheric water vapor [David et al., 2009, 2011; Chwala et al., 2013].

In this paper we present the potential for monitoring of dense fog based on existing Received Signal Level (RSL) measurements from commercial microwave communication networks.

## **2 Method: Fog Identification and Estimation using Measurements from Multiple MLs**

Fog is one of the several atmospheric phenomena that affect MLs, causing an additional signal loss to the microwave electromagnetic beams with respect to that created during non-foggy periods [e.g. Liebe et al., 1989]. Figure 1 presents the theoretical expected attenuation per 1 and 5 km respectively created by fog [Rec. ITU-R P.840-4, 2009], as a function of typical commercial MLs frequencies. These backhaul systems commonly operate in the frequency range between 6 to 40 GHz with bands characteristically at 6, 11, 18, 23, and 38 GHz (Wells, 2009; Frenzel, 2013). The system described is more sensitive to the effects of

fog at the relatively high frequencies. Accordingly, the RSL measurements used in the current work were taken from links operating around the frequency of 38 GHz. The LWC within fogs typically ranges between 0.01 to 0.4 gr/m<sup>3</sup> [Gultepe et al., 2007]. The calculations presented in Fig. 1 were made for different LWC values starting at 0.1 gr/m<sup>3</sup>, and at different temperatures (10 and 15 °C). The maximum values of LWC were taken from field measurements (including five minute average values) carried out in the conducting of recent comprehensive field campaigns in different places in the world, using specialized equipment [Klemm et al., 2005; Herckes et al., 2007; Gultepe et al., 2009; Niu et al., 2010]. The horizontal dashed line indicates the typical measurement resolution of a commercial MLs (links with a coarser measurement resolution exist, but will not be the focus of this paper). We note that for longer links (Fig. 1b), the effective sensitivity per km increases, and lighter fogs can potentially be detected.

Two fundamental stages in fog monitoring using measurements from multiple MLs are distinguished here: identification of the fog phenomenon, and the estimation of its degree using additional standard meteorological instruments (temperature, humidity and rain gauges).

As our primary aim is to prove the feasibility of our proposed methodology, the technique was restricted to situations where other hydrometeors (rainfall, sleet, snow) were nonexistent along the propagation path and we centered our research on extreme fog events.

## 2.1 Fog Identification

We take a set –  $L_1, \dots, L_N$  - of MLs spread across the observed region within the same fog patch. In a typical cellular backhaul network [e.g. Zinevich et al., 2008], microwave links at different lengths and direction exist at an area of a size similar to a dense fog field, e.g. of the

order of several km<sup>2</sup> [e.g. Pagowski et al., 2004]. The availability of diverse RSL measurements enables us to identify the fog induced component with higher statistical precision.

A simplified model describing the attenuation of the *i*-th microwave signal,  $\gamma_i$ , can be described as follows [Zinevich et al., 2010]:

$$\gamma_i = \lfloor A_{fi} + A_{pi} + A_{wi} + A_{vi} + Noise_i \rfloor_{qi} \quad (dB) \quad (1)$$

Where the index *i* signifies the attenuation as measured by the *i*-th ML, let us denote:

$A_{fi}$ - Fog induced attenuation.

$A_{pi}$ - Attenuation as a result of other-than-fog precipitation (rain, sleet, snow).

$A_{wi}$ - Wet antenna attenuation. Because of the high level of humidity during fog, a thin layer of water may accumulate on the outside covers of the microwave antenna and may create additional attenuation to the received signal, beyond that caused by the fog in the atmospheric path.

$A_v$ - Water vapor attenuation

Noise;- All other random signal perturbations, e.g., which created as a result of winds that may oscillate the antennas, variations of the atmospheric refractive index, or temperature variations which may affect the analogue circuitry of the microwave units [Leijnse et al., 2007b; Zinevich et al., 2010].

[ $\lfloor \cdot \rfloor_{qi}$ - Each of the attenuation measurements,  $\gamma_i$ , is quantized according to the given magnitude resolution of each commercial ML.

In this study we assume that  $A_{pi}=0$ . This assumption is validated using nearby standard measurements of rain gauges and temperature meters.

In order to estimate the amount of wet antenna attenuation,  $A_w$ , and if it did in fact occur, we

make use of measurements over particularly short MLs (preferably of up to a few hundreds of meters long) that are located near longer links, since the effect of fog, even a heavy one, as well as of water vapor on the signal attenuation at such short ranges is much smaller comparing to the attenuation created in longer MLs of several km in lengths [Rec. ITU-R P.676-6, 2005; Rec. ITU-R P.840-4., 2009]. This being the case, any additional attenuation, if detected, can be directly attributed to the layer of water on the antennas, its value measured, and that value can be used to adjust the measurements on the longer links.

In order to identify the specific attenuation created as a result of the fog itself, we set a baseline, zero RSL value separately for each link. Since the density of water vapor in the atmosphere affects MLs [Rec. ITU-R P.676-6, 2005; David et al., 2009, 2011] and since humidity is particularly high during fog, the zero level can be chosen by selecting the median value from RSL measurements taken over a period of several hours, during which the relative humidity in the area, as measured by the meteorological stations at the site, is around 90%. Alternatively, since the humidity difference between the foggy day and the reference day is known, the median RSL from the days adjacent to the event can be chosen (e.g. in cases where measurement occurs once daily), and a humidity correction to the baseline is carried out using a known physical model [Rec. ITU-R P.676-6, 2005]. By this selection of the baseline, the water vapor effect,  $A_v$ , is minimized and is assumed to be zero.

Thus, fog is identified as being present when the measured RSL value crosses the predefined threshold during times of high relative humidity (of ~95% and more), while the additional attenuation is observed simultaneously by the numerous MLs spread across the area.

## 2.2 Fog Density Estimation

After detection of the existence of fog, the average amount of LWC per unit of volume in the fog was calculated, from which a rough estimation of the range of visibility was acquired.

### 2.2.1 Liquid water content calculation

At the end of stage 2.1 we are left with the following:

$$\gamma_i = A_{f_i} + A_{w_i} + \tilde{Noise}_i \quad (\text{dB}) \quad (2)$$

We note that the effective noise component as defined here,  $\tilde{Noise}_i$ , includes the contribution from system quantization error.

The relation between the fog induced attenuation,  $A_{f_i}$ , and the total water content per unit volume is given by [Rec. ITU-R P.840-4, 2009]:

$$A_{f_i} = \Phi_i \cdot LWC \cdot L_i \quad (\text{dB}) \quad (3)$$

Where  $L_i$  (km) is link length,  $\Phi_i$  is a frequency and temperature dependent coefficient (known parameters), and  $LWC$  is the liquid water content ( $\text{g m}^{-3}$ ). In this work, we assume that all links deployed across the same fog field observe at the same time the same LWC.

Given  $\gamma_i$  measurements from N links operating around the same frequency and over the same fog patch, the effective fog induced attenuation,  $\hat{a}_f$ , can be extracted from N equations as (4) by a least squares or other estimation method, and provide better accuracy than in the case of measurement from a single link:

$$\gamma_i = \hat{a}_f \cdot L_i + \hat{A}_w + \tilde{Noise}_i \quad (\text{dB}) \quad (4)$$

While:

$$\hat{a}_f = \Phi \cdot LWC \quad (\text{dB/km}) \quad (5)$$

Consequently, the LWC within the fog field is derived through the known relation (5).

$\hat{A}_w$  is the estimated wet antenna component, calculated from the intercept of the linear line with the y-axis.

A mathematical model [ITU-R P.840-4, 2009] based on Rayleigh approximation is used for the calculation of  $\Phi$ , for frequencies of up to 200 GHz (fog drops typically range in size from several microns to a few tens of microns [e.g. Herckes et al., 2007; Gultepe et al., 2009], i.e. small with respect to millimeter microwaves):

$$\Phi = 0.819 f \cdot [\varepsilon''(1 + \beta^2)]^{-1} \quad (\text{dB/km})/(\text{g/m}^3) \quad (6)$$

With  $f$  being the link frequency (GHz), while:

$$\beta = (2 + \varepsilon') / \varepsilon'' \quad (7)$$

The complete expression of the complex dielectric permittivity of water

$\varepsilon(f) = \varepsilon'(f, T) + i\varepsilon''(f, T)$ , is detailed in literature [Rec. ITU-R P.840-4, 2009].

### 2.2.2 Visibility estimation

Visibility is defined as the greatest distance in a given direction at which it is possible to see and identify a prominent black object against the sky at the horizon in the daylight, or the greatest distance it could be seen and recognized during night if the general illumination were raised to the level of normal daylight [WMO, 2008].

In order to estimate the visibility ( $V$ ) we used the following warm- fog visibility parameterization [Gultepe et al., 2006] which takes into account the droplet number

concentration,  $N_D$ , in addition to the LWC:

$$V = 1.002 \cdot (LWC \times N_D)^{-0.6473} \quad (\text{km}) \quad (8)$$

The formula is suitable for warm fog ( $T > 0$  °C) conditions.

$N_D$  can be measured directly using specialized equipment. This value can be estimated given the temperature,  $T$ , by using the following known relation [Gultepe and Isaac, 2004]:

$$N_D = -0.071T^2 + 2.213T + 141.56 \quad (\text{cm}^{-3}) \quad (9)$$

We acquire a rough range of  $V$  based on maximum and minimum bounds derived from the uncertainty in estimating this parameter.

### 3 Uncertainty and bounds on the visibility estimate

#### 3.1 Water vapor effect

Spatio-temporal variations in water vapor concentration (e.g. Fabry, 2006) affect the chosen baseline for calculating the fog induced attenuation for each one of the links. Figure 2 presents the theoretical expected attenuation per 1 km (Fig. 2a) and 5 km (Fig.2b) created by different water vapor densities, as a function of the typical commercial MLs frequencies. The calculation was made for a temperature of 15 °C in the humidity range between 25% and 100% which matches a water vapor concentration of between 3 and 13 gr/m<sup>3</sup>, respectively, at sea level pressure (Rec. ITU-R P.676-6, 2005). A noticeable absorption line can be seen around the 22.2 GHz range (Van Vleck, 1947). We chose the 38 GHz band where the sensitivity to fog is the highest in the given range (Fig. 1). This choice is also advantageous since it is diverted from the absorption line (22.2 GHz) where humidity induced attenuation is

dominant (David et al., 2009, 2011; Chwala et al., 2013).

The effect of water vapor on the baseline RSL chosen can be estimated by the difference between the expected attenuation curve under fog conditions (the 100% curve) and the humidity state at the time the reference measurements were taken (the 75% curve, representing a typical value for the conditions that were measured). This difference, at 38 GHz, is in the range between 0.05 and 0.3 dB for links of 1 and 5 km lengths, respectively. These values are of a lower order of magnitude with respect to the expected attenuation from high concentration fog (Fig. 1). Nevertheless, we made a water vapor correction to the chosen RSL value according to the difference in the curves calculated for each link, using side information from the humidity gauges.

### 3.2 Liquid water content

The dominant source of uncertainty in estimating the LWC is the uncertainty in estimating the effective fog induced attenuation,  $\hat{a}_f$ . In order to estimate the error in this value we used the error estimation formula for a linear slope [Kenney and Keeping, 1962]:

$$\Delta\hat{a}_f = \sqrt{\sum_1^n (\gamma_i - \hat{\gamma}_i)^2 \cdot \left[ (n-2) \cdot \sum_1^n (L_i - \bar{L})^2 \right]^{-1}} \quad (dB/km) \quad (10)$$

Where:

$n$  – Number of samples

$\gamma_i$  – The attenuation measured by the  $i$ -th link

$\hat{\gamma}_i$  – The attenuation estimated by the linear approximation for the  $i$ -th link

$L_i$  – Length of the  $i$ -th link

$\bar{L}$  – Average length of the links

Based on Eq. (5), uncertainty in estimating attenuation leads to uncertainty in the LWC

estimation which is given by [Ku, 1966]:

$$\Delta LWC = \Delta \hat{a}_f \cdot \Phi^{-1} \quad (gr/m^3) \quad (11)$$

In this study, the uncertainty caused due to temperature variations was neglected while deriving Eq. (11). The difference between the temperature measurements of the different gauges (with an instrument error of 0.1 °C) in the observed area was between 1 and 2 °C at the time of the microwave system measurement. This uncertainty creates LWC variations an order of magnitude less than the uncertainty created from the effective fog induced attenuation using the model [Rec. ITU-R P.840-4, 2009].

### 3.3 Wet antenna

The estimation of attenuation resulting from a possible wet antenna,  $A_w$ , was carried out by evaluating the y-intercept of the line (which represents a theoretical distance of 0 between the antennas). In order to estimate the error in this value we used the calculation for constant term error in a linear approximation [Kenney and Keeping, 1962]:

$$\Delta \hat{A}_w = \sqrt{\sum_1^n (\gamma_i - \bar{\gamma}_1)^2 \sum_1^n L_i^2 \cdot \left[ n(n-2) \cdot \sum_1^n (L_i - \bar{L})^2 \right]^{-1}} \quad (dB) \quad (12)$$

### 3.4 Visibility estimate bounds

Since LWC is highly correlated to visibility, several empirical models were developed to estimate one quantity given the other [e.g. Tomasi and Tampieri, 1976; Pinnick et al., 1978; Kunkel, 1984; Klemm et al., 2005; Acker et al., 2010]. Of these, the model developed by Kunkel [1984] is commonly used for visibility estimations in many prediction models [e.g. Benjamin et al., 2004; Terradellas and Bergot, 2007]. However, environmental conditions and the microphysical structure of fog also affect the visibility. Previous studies have shown that for a certain, constant, LWC level, visibility can vary [e.g. Klemm et al., 2005].

Specifically, other research has indicated the dependence of visibility on  $N_D$ . For example, Meyer et al. [1980], show that visibility is a function of  $N_D$  and varies with fog intensity. Thus, taking  $N_D$  into account will allow visibility estimations with higher precision to be obtained. The warm-fog visibility parameterization developed by Gultepe et al. [2006] includes this parameter in addition to the LWC (Eq. (8)).

We set an upper and lower rough bound for the visibility assessment based on the contribution from two factors – the LWC uncertainty derived directly from the link measurements, and from an assumed uncertainty which was taken to be 30% for the warm-fog visibility parameterization. Prior research [Gultepe et al., 2006] has shown that the uncertainty estimation for Eq. (8) is about 29%, where the uncertainties in LWC and the parameter  $N_D$  taken into account in creating this estimate were 15% and 30% respectively, and under the assumption that in visibility, fractional uncertainty is the sum of the fractional uncertainties in LWC and the parameter  $N_D$ . While this uncertainty shows there is still room for improvement, it is nonetheless more accurate than the Kunkel [1984] model, which, depending on environmental conditions, over/under-estimated visibility by more than 50% [Gultepe et al, 2006]. The formula was derived based on LWC in the range between 0.005 and 0.5  $\text{gr}/\text{m}^3$  and for values of  $N_D$  between 1 and about 400 ( $\text{cm}^{-3}$ ). We note that the estimation of  $N_D$  in this paper was derived from the temperature (Eq. (9)), which may create additional disparities in estimating this parameter [Gultepe and Isaac, 2004; Gultepe et al., 2006] due to dependency on other physical and dynamic factors (e.g., nucleation and turbulence, respectively). To reach the visibility range presented here, first, the maximum and minimum values of LWC observed by the links were calculated, according to the uncertainty values associated with calculating LWC from attenuation measurements (Eq. (11)). Then, the visibility range was calculated from these minimum and maximum LWC values using Eq. (8) and assuming a 30% uncertainty estimate related to this calculation [Gultepe et al., 2006].

Based on these assumptions, in this paper, we note that the estimated visibility range is a measure of an order of magnitude. Adding information about the microphysical structure of the fog based, for example, on side information taken by proprietary instruments (e.g. direct measurement of  $N_D$ ) will reduce the uncertainty in the visibility estimate, which is a matter for future research.

#### **4 Results**

We centered our research on two extreme fog events that took place in Israel. In both cases visibility dropped to or below several tens of meters, and the events continued throughout the night and the following morning. The thick fog developed to a scale of a few tens of km, covered the southern and central coastal plain and lowland regions of Israel as well as parts of the Sinai Peninsula in Egypt, as illustrated by the satellite images (Fig. 3a, Fig. 6a). The images were produced using CAPSAT- the Clouds-Aerosols-Precipitation Satellite Analysis Tool [Lensky and Rosenfeld, 2008] based on infrared measurements from a combination of 3 of the SEVIRI (spinning enhanced visible and infrared imager) channels (IR3.9, IR10.8 and IR12.0). The extremely low visibility conditions during these fog events led to disruption, cancellations and delays in the flight schedule for Ben Gurion international airport.

Our analysis focuses on the central western coastal region (Tel- Aviv city- Ben Gurion airport area) where several means for measuring the phenomenon exist. The microwave data used was gathered from the tens of commercial MLs operating at around the 38 GHz frequency range in the area that are located in the vicinity of the specialized measuring equipment. The links are installed at elevations between 5 and 90 m Above Sea Level (ASL), on towers that range from 5 to 100 meters Above Ground Level (AGL) and span in length from 100 m to ~3.5 km. Each one of the links provides one measurement per day at a 0.1dB resolution. The measurements are taken instantaneously and simultaneously across all of the links in the

system at a prescribed time as reported by the cellular providers. During both events, no rainfall, sleet or snow were measured in the examined area according to the observations of the surface stations.

#### **4.1 Case 1: 9-10 December 2005**

Between the late evening of 9 December 2005 and the morning hours of the next day, a heavy fog front passing through central Israel was recorded by different observation techniques found in the area. At the surface, a ridge from the west with weak westerlies (and a long fetch over the Mediterranean Sea) was accompanied by a deep ridge aloft, which was causing significant subsidence.

Since the microwave system that provided the data used for this research recorded measurements around 01:30 we used this time frame as the focal point for our research (all hours are in Universal Time Coordinated).

Figure 3a shows the regional satellite image acquired during the event (01:27). Figure 3b indicates the location of the different measuring means in the region as well as the deployment of the ML system. According to the measurements of the three regional stations in the observed area (Fig. 3b), the Relative Humidity (RH), as measured between 01:00 and 02:00, ranged between 97%-100%. (with temperature of around +13 °C and wind speed of ~1-2.5 m/s).

Visibility assessments were acquired by two human observers located at the Beit Dagan station, and at the Ben Gurion airport (Fig. 4a). The Meteorological Optical Range (MOR) measurements [WMO, 2008] were taken by the three transmissometers located at the airport (Fig. 4b). According to these different observation techniques limited visibility due to fog was detected between 22:00 and 07:00 (of 9- 10 December, respectively), dropping to a

minimum of 50 m (transmissometers) and 100 m (Ben Gurion observer).

#### **4.1.1 Fog identification and intensity estimation using MLs measurements**

We used 88 MLs in the observed region during the event, deployed over 47 different paths, covering an area of approximately 5 by 6 km<sup>2</sup> (Fig. 3b). Each of the links provided one measurement every 24 hours (01:30). We compared attenuation measurements from the foggy night to those taken on a humid night without fog (according to the records from the different specialized measuring instruments).

**1. Fog Identification:** During the foggy night, on 10 December 2005, an RSL drop was recorded by numerous MLs, of different lengths, located in the area (during RH >95% conditions). Figure 5a presents the attenuation measurements from the different MLs, as a function of link length. Figure 5b shows the measurements which were acquired during a humid night (15 December) without fog (a RH of ~65%, ~90% and 85% was measured by the Tel Aviv coast, central Tel Aviv, and Beit Dagan surface stations around 01:30). The additional attenuation measured by the links on the foggy night with respect to the humid night is apparent. During the foggy night the Pearson correlation coefficient between observed attenuation to link length was found to be  $r=0.55$  (with P-value < 0.01 [Neter et al., 1996], based on 88 data points).

Given the high RH of ~95% and the additional attenuation observed by the multiple MLs, fog was identified as being present in the area.

## 2. Estimating liquid water content and visibility

The estimate of the effective fog induced attenuation-  $\hat{a}_f$ , is given by the slope of the resulting plot (Fig. 5a). The estimate for the wet antenna component,  $\hat{A}_w$ , is given by the constant term.

A similar plot was created for the non foggy night, where the slope of the resulting graph tends to zero (Fig. 5b).

Given,  $\hat{a}_f$ , the temperature and the MLs frequency we calculated the value for the LWC using Eq. (5). Then, minimum and maximum bounds on the range of visibility were derived using Eqs. (8) to (11). The resulting values were  $0.7 \pm 0.1 \text{ gr/m}^3$  and 30 to 70 m, respectively.

Table 1 lists the results of the ML measurements and the visibility assessments received, during the same time period, from the different measurement means.

The visibility assessments derived from the ML measurements are of a similar order of magnitude as the assessments from the specialized measurement equipment.

### 4.2 Case 2: 15-16 November 2010

Starting on the evening of 15 November 2010, a heavy fog front began developing and expanding along the area of Israel's Mediterranean coast. At the surface, a Red Sea Trough with a central axis was moving eastward, allowing for northwesterly flow from the Mediterranean Sea to move into the coastal area. Aloft, a deep ridge was moving eastward. Fog conditions continued through the morning hours of 16 November 2010.

The satellite image shows the wide region affected during this fog event (Fig. 6a), as well as the site discussed here, which is detailed in the map (Fig. 6b) adjacent to the image.

The microwave system that provided the data used for this research recorded measurements at 22:00 and hence we used this time frame as the focal point for our research.

We focused on the area of Beit Dagan station (Fig. 6b) in the proximity of MLs where the measured humidity was 90% - 97% between 21:30 and 22:30 (with a temperature range of 18.5 -19 °C and wind speed of ~1 to ~3 m/s). Figure 7a shows the visibility results registered by the professional human observers located at Beit Dagan station and Ben Gurion airport. The graphs described in Fig. 7b are based on Runway Visual Range (RVR) measurements [AMS, 2000] of three transmissometers located at the airport. In addition, MOR measurements of a scattermeter found at Beit Dagan which was available during this event, are also presented.

According to all of these observations, between 21:30 and 07:30 of 15-16 November 2010 severe visibility limitations were observed, decreasing to the order of a few tens of meters and less (between 22:00 and 01:00).

#### **4.2.1 Fog identification and intensity estimation using MLs measurements**

58 MLs deployed in the observed region over 39 separate paths were used during the event (Fig. 6b). The system is spread across an area of approximately 10 x 15 km<sup>2</sup>, and captures one instantaneous measurement from each link every night (at 22:00). We compared the measurements taken on the foggy night to those taken during a humid night at the same hour.

**1. Fog Identification:** During the foggy night (15 November), an RSL drop was recorded by multiple MLs located in the area (at RH of ~95%). The attenuation measurements from the ML network in the area during this night are presented in Fig. 8a. The correlation between observed attenuation and link length during the foggy night was  $r = 0.57$  (P-value < 0.01,

based on 58 data points). Figure 8b shows the measurements taken on a humid night (10 November) without fog (RH ~87% around 22:00, according to Beit Dagan station).

Given the high RH of ~95% and the additional attenuation observed by the multiple MLs fog was identified as being present in the area.

**2. Estimating liquid water content and visibility:** The LWC value measured, using the same procedure described previously, was found to be  $0.68 \pm 0.15 \text{ gr/m}^3$ . Accordingly, the range of visibility was assessed to be 30 to 70 m.

Table 2 lists the ML measurements and the different visibility assessments as measured around 22:00 by the different measurement means.

## 5 Discussion

The physical effects of fog on radiation in the microwave range are well studied [e.g. Liebe et al., 1989; Rec. ITU-R P.840-4, 2009; Csurgai-Horváth and Bitó, 2010]. The novelty of the work presented here is the concept of using *existing* commercial microwave infrastructure, as a fog detection tool, for measuring LWC and deriving visibility assessments. The challenges in fog monitoring using commercial MLs are mostly due to the fact that system measurements are optimized for communication quality of service, and not for meteorological observations, so factors such as link frequency, temporal resolution or quantization of the measurements are given. The opportunities come, on the other hand, from the availability of many links. These are widely spread across the terrain at relatively high densities and different lengths/heights, observing the atmospheric phenomenon simultaneously at various frequencies.

Our results show that these systems have a potential for fog monitoring, especially in cases of heavy fog that creates severe visibility limitations particularly as it drops to the tens of meters

range.

The liquid water content values calculated from the microwave system measurements match similar high values measured directly in field studies, particularly when taking into account the error range in microwave measurements. Values above  $0.5 \text{ gr/m}^3$  were observed in several recent studies during periods of dense fog [e.g. Klemm et al., 2005; Herckes et al., 2007; Gultepe et al., 2009; Niu et al., 2010].

The visibility assessments calculated using the proposed method are of the same order of magnitude as the values measured directly by the different visibility measuring instruments and human observers during the same time period.

Environmental and technical factors are both sources of error in estimating the fog induced attenuation [Leijnse et al., 2007b; Zinevich et al., 2010]. Environmental factors include: spatial variation of the fog, variation in the atmospheric refraction index, condensation of dew on the antenna radomes and scatterers in proximity to the propagation path (e.g. fluttering tree leaves). Technical factors may be ascribed to e.g. system quantization and white noises, the effect of temperature changes on the analog circuits of the radio. All these directly affect the chosen reference baseline for a specific link. Another potential source of error is the possibly wetting of the antenna during a fog event. The wet antenna effect is well known as a main source of error when measuring rainfall using a ML [e.g. Leijnse et al., 2008; Zinevich et al., 2010; Schleiss et al., 2013]. However, in our case the source of possible wettings is different comparing to the case of rainfall since it is resulting from condensation of the atmospheric water vapor due to the high RH. Our results suggest that this effect is likely to be considerable also in the case of fog monitoring using MLs. We note that the wetness on one radio unit might be different from that on a different unit due to differing atmospheric conditions, antenna elevations, etc. As a result, this phenomenon might cause different attenuation levels from link to link, and add to the uncertainty in the measurements.

On the other hand, a positive contribution of this wet antenna component is that it may be utilized as an additional fog detection factor. In order to reduce the measurement errors resulting from these different factors, we utilized the availability of multiple measurement sources, and the diversity of such sources, based on the availability inherent in the nature of typical communication systems. Particularly, we were able to derive an estimate for the wet antenna attenuation, and reduced the sources of random error. More research is needed regarding these issues in future work.

During this study we used a system that provided one measurement every 24 hour period. The measurements were collected from several tens of links in a bounded area of several square kilometers. This way of deriving the observed value, may reduce the spatial resolution in the specific closed area, but on the other hand, the representativeness of the measurement is greater, particularly when compared to those measured by specialized instruments, which are located at a single point, and are especially problematic from this point of view [Gultepe et al., 2007]. One should note that, commercial systems with higher temporal resolution measurement exist e.g. systems that provide measurements every minute, or every 15 minutes [e.g. Goldshtein et al., 2009; David et al., 2013]. Additionally, MLs also operate at higher frequencies, e.g. around 60 or 80 GHz [e.g. Wells, 2009]. It is therefore expected that using higher resolution measurement systems to observe the phenomenon will improve the measurements and the ability to track lighter fogs.

Two fog events were investigated in the current study. Further research is required in order to assess the viability of the proposed method in the general case, beyond the events presented here. For example, a large number of events in different condition ranges and from different geographical regions need to be analyzed, as well as the need for, and dependence on, meteorological side information. Measurement precision, and particularly that of the LWC, should further be researched and estimated, while comparing to measurements from

specialized reference instruments. Adding information about the microphysical characteristics of the fog in addition to LWC into the model will also allow for improvements in the visibility estimates [Meyer et al., 1980, Gultepe et al., 2006, Niu et al., 2010]. The aim of this study is to provide a proof of concept of the described system's potential to monitor the phenomenon and these issues are left to future research.

Beyond the positive benefits of fog, this phenomenon poses a danger, particularly in cases of heavy fog that leads to disruptions and accidents in different transportation realms. MLs, which form the infrastructure of cellular communication networks, are widely deployed and exist in most places around the globe. Use of the proposed method does not require additional expenses or installation of special equipment beyond standard meteorological measurements. On the other hand, application of the proposed technique can contribute to the better understanding of fog related processes, as well as to the development of parameterizations for numerical weather prediction models. Furthermore, the potential of the system for monitoring the phenomenon and providing real time warning of it is great.

*Acknowledgments.* The authors are grateful to Y. Dagan, Y. Eisenberg (Cellcom), A. Shilo and N. Dvella (Pelephone) for providing the microwave data for our research. We wish to thank the Israel Meteorological Service (IMS), Meteotech and the Ministry of Environmental Protection for meteorological data. In addition, we would like to acknowledge and thank our current and former research team members (Tel Aviv University): A. Rayitsfeld, Dr. A. Zinevich, U. Hadar, Y. Ostrometzky, R. Samuels, D. Cherkassky, O. Auslender, R. Radian for their advice and assistance throughout the research. We also wish to thank EUMETSAT for satellite data. A special thank to I. Lensky (BIU) for providing satellite image processing software. This research was supported by the Israel Science Foundation (grant No. 173/08) and also by Grant No. 2010342 from the United States- Israel Binational Science Foundation (BSF).

This paper is presented in partial fulfillment of the requirements for the degree of Doctor at Tel Aviv University.

## References

Acker, K., W. Wiegand, D. Kalass, D. Möller, and P. Chaloupecky, (2010), Relationship between liquid water content and visibility in low clouds occurred at Mt. Brocken, International Aerosol Conference (IAC), Helsinki.

Arends, B.G., G.P.A. Kos, W. Wobrock, D. Schell, K. J. Noone, S. Fuzzi, and S. Pahl (1992), Comparison of techniques for measurements of fog liquid water content, *Tellus*, 44B, 604-611.

Benjamin, S. G., D. Devenyi, S. S. Weygandt, K. J. Brundage, J. M. Brown, G. A. Grell, D. Kim, B. E. Schwartz, T. G. Smirnova, T. L. Smith, and G. S. Manikin (2004), An hourly assimilation–forecast cycle: The RUC, *Mon. Weather. Rev.*, 132, 495–518.

Croft, P. J., D. Darbe, and J. Garmon (1995), Forecasting significant fog in southern Alabama, *Natl. Wea. Dig.*, 19, 10–16.

Chwala, C., A. Gmeiner, W. Qiu, S. Hipp, D. Nienaber, U. Siart, T. Eibert, M. Pohl, J. Seltmann, J. Fritz, and H. Kunstmann (2012), Precipitation observation using microwave backhaul links in the alpine and pre-alpine region of Southern Germany, *Hydrol. Earth Syst. Sci.*, 16, 2647-2661, doi:10.5194/hess-16-2647-2012.

Chwala, C., H. Kunstmann, S. Hipp, and U. Siart (2013), A monostatic microwave transmission experiment for line integrated precipitation and humidity remote sensing, *Atmos. Res.*, doi: 10.1016/j.atmosres.2013.05.014.

-, L., and J. Bitó (2010), Fog attenuation on V band terrestrial radio and a low-cost measurement setup, In *Future Network and Mobile Summit, 2010*, IEEE.

Dam, D. A., and X. C. Hoang (2008), Nguyen T.K.O. Photochemical smog introduction and episode selection for the ground-level ozone in Hanoi, Vietnam, *VNU Journal of Science, Earth Sciences*, 24, 169-175.

David, N., P. Alpert, and H. Messer (2009). Technical Note: Novel method for water vapour monitoring using wireless communication networks measurements, *Atmos. Chem. Phys.*, 9, 2413-2418.

David, N., P. Alpert, and H. Messer (2011). Humidity measurements using commercial microwave links, *Advanced Trends in Wireless Communications*, InTech publications, Croatia, 65-78.

David, N., P. Alpert, and H. Messer (2013). The potential of cellular network infrastructures for sudden rainfall monitoring in dry climate regions, *Atmos. Res.*, 131, 13-21, doi: 10.1016/j.atmosres.2013.01.004.

Dawson, T. E. (1998), Fog in the California redwood forest: ecosystem inputs and use by plants, *Oecologia*, 117, 476–485.

Ellrod, G. P. (1995), Advances in the detection and analysis of fog at night using GOES multispectral infrared imagery, *Wea. Forecasting.*, 10, 606–619.

Ellrod, G. P., and I. Gultepe (2007). Inferring low cloud base heights at night for aviation using satellite infrared and surface temperature data, *Pure Appl. Geophys.*, 164, 1193-1205.

Emert, S. E. (2001), Design, construction and evaluation of the CSU optical fog detector, M.Sc thesis, Colorado State University, Fort Collins, Colorado.

Fabry, F. (2006), The spatial variability of moisture in the boundary layer and its effect on convection initiation: Project-long characterization, *Mon. Wea. Rev.*, 134, 79–91, doi: 10.1175/MWR3055.1.

Frenzel, L.E. (2013), Millimeter waves will expand the wireless future, *Electron. Des. Mag.*, 30-36.

Gerber, H. (1984), Liquid water content of fogs and hazes from visible light scattering, *J.*

Climate Appl. Meteor., 23, 1247-1252.

Glickman, T. S. (2000), American Meteorological Society (AMS): glossary of meteorology, 2nd edition, Allen Press.

Goldshstein, O., H. Messer, and A. Zinevich (2009). Rain Rate Estimation Using Measurements From Commercial Telecommunications Links, IEEE Trans. Signal Process., 57, 1616-1625.

Gultepe, I., and G. A. Isaac (2004), Aircraft observations of cloud droplet number concentration: Implications for climate studies, Q. J. R. Meteorolog. Soc., 130, 2377–2390.

Gultepe, I., M. D. Müller, and Z. Boybeyi (2006), A new visibility parameterization for warm-fog applications in numerical weather prediction models, J. Appl. Meteor. Climatol., 45, 1469–1480.

Gultepe, I., R. Tardif, S. C. Michaelides, J. Cermak, A. Bott, J. Bendix, M. D. Muller, M. Pagowski, B. Hansen, G. Ellord, W. Jacobs, and G. Toth, S. G. Cober (2007), Fog research: a review of past achievements and future perspectives, Pure Appl. Geophys., 164, 1121–1159.

Gultepe I., G. Pearson, J. A. Milbrandt, B. Hansen, S. Platnick, P. Taylor, M. Gordon, J. P. Oakley, and S. G. Cober (2009), The fog remote sensing and modeling field project. Bull. Amer. Meteor. Soc., 90(3), 341–359.

Herckes, P., H. Chang, T. Lee, and J. L. Collet (2007), Air pollution processing by radiation fogs, Water Air Soil Poll., 181, 65–75.

Kenney, J. F., and E. S. Keeping (1962), Linear regression and correlation. Van Nostrand Publishers, Princeton, N.J., 252-285.

Klemm, O., T. Wrzesinsky, and C. Scheer (2005), Fog water flux at a canopy top: direct measurement versus one-dimensional model, Atmos. Environ., 39, 5375-5386.

Klemm, O., R. S. Schemenauer, A. Lummerich, P. Cereceda, V. Marzol, D. Corell, J. Van Heerden, D. Reinhard, T. Gherezghiher, J. Olivier, P. Osses, J. Sarsour, E. Frost, M. J. Estrela, J. A. Valiente, and G. M. Fessehaye (2012), Fog as a fresh-water resource: overview and perspectives, *AMBIO*, 41, 221-234.

Ku, H. H. (1966), Notes on the use of propagation of error formulas. *J. Res. Nbs. C. Eng. Inst.*, 70, 263-273.

Kunkel, B. (1984), Parameterization of droplet terminal velocity and extinction coefficient in fog models, *J. Appl. Meteor. Climatol.*, 23, 34-41.

Leijnse, H., R. Uijlenhoet, and J. Stricker (2007a), Rainfall measurement using radio links from cellular communication networks, *Water Resour. Res.*, 43, W03201, doi: 10.1029/2006WR005631.

Leijnse, H., R. Uijlenhoet, and J. Stricker (2007b), Hydrometeorological application of a microwave link: 1. Evaporation. *Water Resour. Res.* 43, W04416, doi: 10.1029/2006WR004988.

Leijnse, H., R. Uijlenhoet, and J. Stricker (2008), Microwave link rainfall estimation: Effects of link length and frequency, temporal sampling, power resolution and wet antenna attenuation, *Adv. Water Resour.* 31, 1481-1493, doi:10.1016/j.advwatres.2008.03.004.

Lensky, I. M. and D. Rosenfeld (2008), Clouds-Aerosols-Precipitation Satellite Analysis Tool (CAPSAT), *Atmos. Chem. Phys.*, 8, 6739-6753, doi:10.5194/acp-8-6739-2008.

Liebe, H. J., T. Manabe, and G. A. Hufford (1989), Millimeter-wave attenuation and delay rates due to fog/cloud conditions, *IEEE T. Antenn. Propag.*, 37(12), 1617-1612.

Messer, H., A. Zinevich, and P. Alpert (2006), Environmental monitoring by wireless communication networks, *Science*, 312, 713.

Meyer, M. B., J. E. Jiusto, and G. G. Lala.(1980), Measurements of visual range and

radiation-fog (haze) microphysics, *J. Atmos. Sci.*, 37, 622–629.

Niu, S. J., C. S. Lu, L. J. Zhao, J. J. Lu, and J. Yang (2010b), Analysis of the microphysical structure of heavy fog using a droplet spectrometer: a case study, *Adv. Atmos. Sci.*, 27(6), 1259-1275, doi:10.1007/s00376-010-8192-6.

Neter, J., M. H. Kutner, C. Nachtsheim, and W. Wasserman (1996), *Applied Linear Statistical Models*, 4th Edition, McGraw Hill, Inc., 640–645.

Oliver, J. (2004), Fog harvesting: An alternative source of water supply on the West Coast of South Africa, *GeoJournal*, 61, 203–214.

Pagowski, M., I. Gultepe, and P. King (2004), Analysis and modeling of an extremely dense fog event in southern Ontario, *J. Appl. Meteor.*, 43, 3–16.

Pinnick, R. G., D. L. Hoihjelle, G. Fernandez, E. B. Stenmark, J. D. Lindberg, and G. B. Hoidale (1978), Vertical structure in atmospheric fog and haze and its effects on visible and infrared extinction, *J. Atmos. Sci.*, 35, 2020-2032.

Pisano, P. A., L. C. Goodwin, and M. A. Rossetti (2008), U.S. highway crashes in adverse road weather conditions, Proceedings of the 88th Annual American Meteorological Society meeting, New Orleans, L.A., U.S.A, 20-24 January, 1-15.

Rayitsfeld, A., R. Samuels, A. Zinevich, U. Hadar, and P. Alpert (2011), Comparison of two methodologies for long term rainfall monitoring using a commercial microwave communication system, *Atmos. Res.*, 104-105, 119-127.

Rec. ITU-R P.838-2 (2004), Specific attenuation model for rain for use in prediction methods.

Rec. ITU-R P.676-6 (2005), Attenuation by atmospheric gases.

Rec. ITU-R P.840-4 (2009), Attenuation due to clouds and fog.

- Schleiss, M., J. Rieckermann, and A. Berne (2013), Quantification and modeling of wet antenna attenuation for commercial microwave links, *IEEE Geosci. Remote Sens. Lett.*, 10, 1195-1199.
- Schwarzenboeck, A., G. Mioche, A. Armetta, A. Herber, and J. F. Gayet (2009), Response of the Nevzorov hot wire probe in clouds dominated by droplet conditions in the drizzle size range, *Atmos. Meas. Tech.*, 2, 779-788, doi:10.5194/amt-2-779-2009.
- Tago., H., H. Kimura, K. Kozawa, and K. Fujie (2006), Long-term observation of fogwater composition at two mountainous sites in Gunma Prefecture, Japan, *Water Air Soil Pollut.*, 175, 375-391.
- Terradellas, E., and T. Bergot (2007), Comparison between two single-column models designed for short-term fog and low-clouds forecasting, *Física Tierra*, 19, 189–20.
- Tomasi, C., and F. Tampieri (1976), Features of the proportionality coefficient in the relationship between visibility and liquid water content in haze and fog, *Atmosphere*, 14, 61–76.
- Van Vleck, J.H. (1947), Absorption of microwaves by uncondensed water vapor, *Phys. Rev.*, 71, 425- 433.
- Wang, Z., M. Schleiss, J. Jaffrain, A. Berne, and J. Rieckermann (2012), Using Markov switching models to infer dry and rainy periods from telecommunication microwave link signals, *Atmos. Meas. Tech.*, 5, 1847-1859, doi:10.5194/amt-5-1847-2012.
- Wells, J. (2009), Faster than fiber: the future of multi-G/s wireless, *IEEE Microw. Mag.*, 10, 104-112.
- Wichmann, H. E., W. Mueller, P. Allhoff, M. Beckmann, N. Bocter, M. J. Csicsaky, M. Jung, B. Molik, and G. Schoeneberg (1989), Health effects during a smog episode in West Germany in 1985, *Environ Health Perspect*, 79, 89–99.

WMO- World Meteorological Organization (2008), Guide to meteorological instruments and methods of observation, 7th edition, ISBN 978-92-63-10008-5.

Wrzesinsky, T., and O. Klemm (2000), Summertime fog chemistry at a mountainous site in central Europe, *Atmos. Environ.*, 34, 1487-1496.

Zinevich, A., P. Alpert, and H. Messer (2008), Estimation of rainfall fields using commercial microwave communication networks of variable density, *Adv. Water Resour.*, 31, 1470-1480.

Zinevich, A., H. Messer, and P. Alpert (2009), Frontal rainfall observation by a commercial microwave communication network, *J. Appl. Meteor. Climatol.*, 48, 1317-1334.

Zinevich, A., H. Messer, and P. Alpert (2010), Prediction of rainfall intensity measurement errors using commercial microwave communication links, *Atmos. Meas. Tech.*, 3, 1385-1402.

Accepted Article

**Table 1.** Comparison of the visibility assessments and microwave measurements with the specialized measurement instruments (10 December 2005). The observations listed in the table were made over the same time when the ML measurements were taken, where the hour / time period indicated in parentheses in each column is the period during which the measurement was taken by each mean (the visibility range based on ML measurements indicates the upper and lower bound for the estimate). Temperature and RH measurements were acquired (at 10-minute intervals) by the three ground stations between 01:20 and 01:40. The Ben Gurion and Beit Dagan observers provided visibility estimates once an hour and once every 3 hours, respectively. The MOR measurements are based on 10-minute intervals as acquired by each of the three transmissometers. The LWC, wet antenna and fog induced attenuation values measured by the MLs, are also listed.

RH [%]	T [°C]	$\hat{A}_w$ [dB]	$\hat{a}_f$ [dB/km]	LWC [gr/m <sup>3</sup> ]	MLs Vis max/min bounds [m]	MOR [m] (B. Gurion)	B. Gurion Observer [m]	B. Dagan Observer [m]
97- 100	12-13.5	0.62±0.15	0.63±0.1	0.7± 0.1	30-70 (01:30 h)	~50 (01:20- 01:40 h)	100-400 (01:00- 02:00 h)	500- 900 (00:00- 03:00 h)

**Table 2:** Comparison of the visibility assessments and microwave measurements with the specialized measurement instruments (15 November 2010). The observations listed in the table were made over the same time when ML measurements were taken, where the hour / time period indicated in parentheses in each column is the period during which the measurement was taken by each measuring mean. Temperature and RH measurements were acquired by the Beit Dagan ground station between 21:50 and 22:10 (at 10-minute intervals). Observers provided visibility estimates once an hour. The MOR measurements were taken by the scattermeter at Beit Dagan, in 1 minute intervals. The notation “Med” indicates the median value.

RH [%]	T [°C]	$\hat{A}_w$ [dB]	$\hat{a}_f$ [dB/km]	LWC [gr/m <sup>3</sup> ]	MLs Vis max/min bounds [m]	MOR [m] (B. Dagan)	B. Gurion Observer [m]	B. Dagan Observer [m]
90-96	19	0.21±0.15	0.53±0.1	0.68± 0.15	30- 70  (22:00 h)	30 to 950  Med= 70  (21:50- 22:10 h)	50-500  (22:00- 23:00 h)	Several  meters-100  (22:00- 23:00 h)

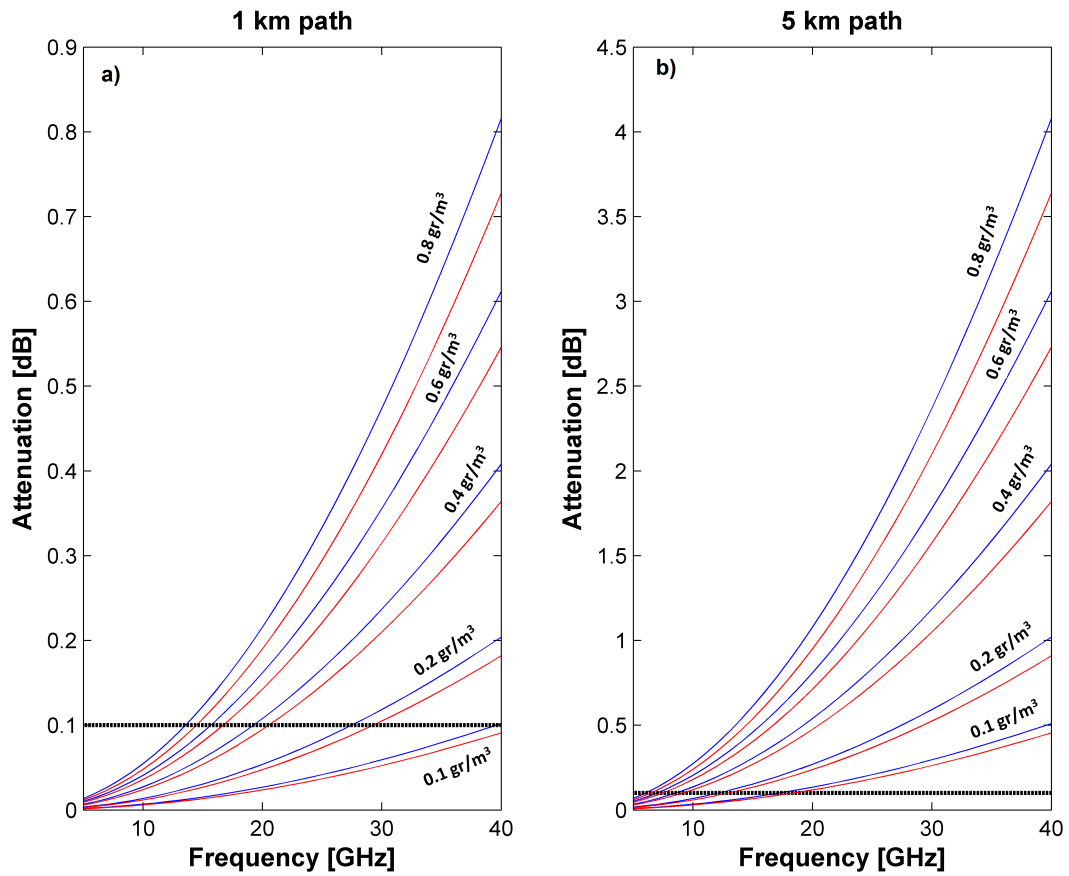


**Figure 1.** Transmission loss due to fog. Signal attenuation per 1 km (a) and 5 km (b) created by different levels of fog concentration at temperatures of 15 (red) and 10 (blue) °C, as a function of the ML operating frequency. The dashed line (black) indicates a typical measurements resolution of commercial MLs (0.1 dB). Given a certain LWC value, the expected attenuation is greater for higher frequencies, at lower temperatures.

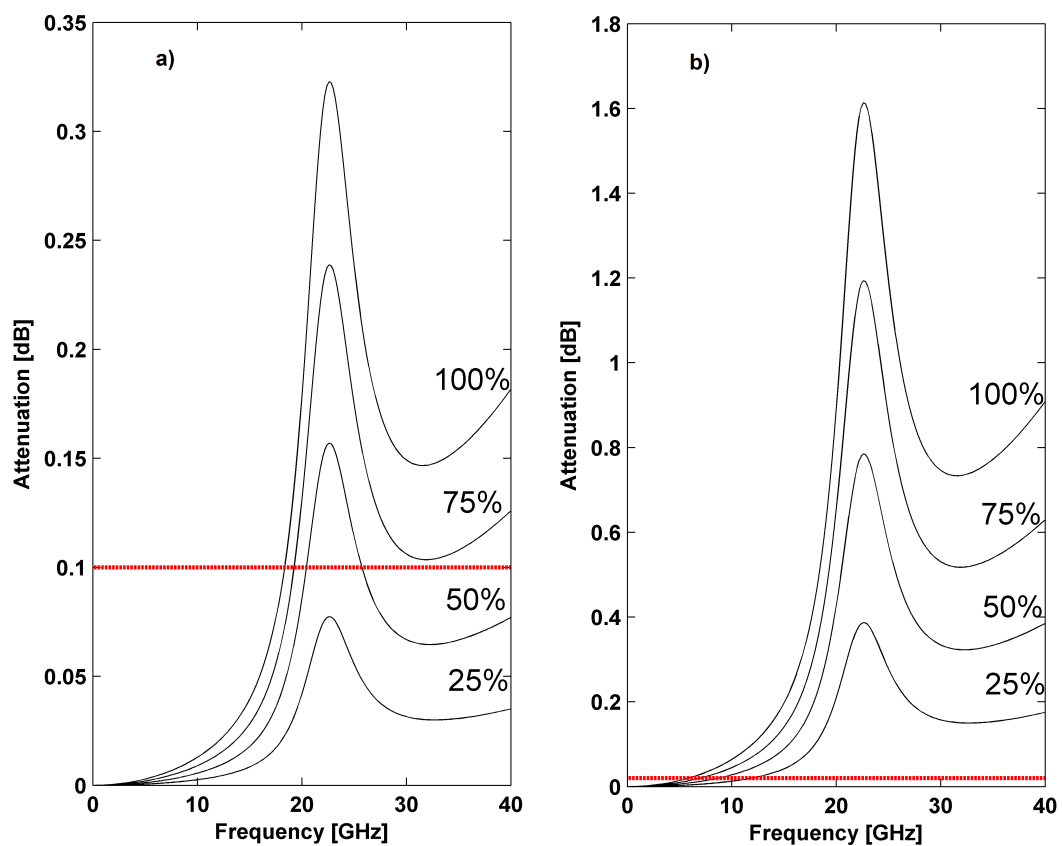


**Figure 2.** Transmission loss due to water vapor. The percentages indicate relative humidity. The horizontal line (red) indicates the typical magnitude resolution of a commercial microwave link, and specifically that of the system used for this research (0.1dB). The attenuation values shown are calculated from approximations to the model (Rec. ITU-R P.676-6, 2005).

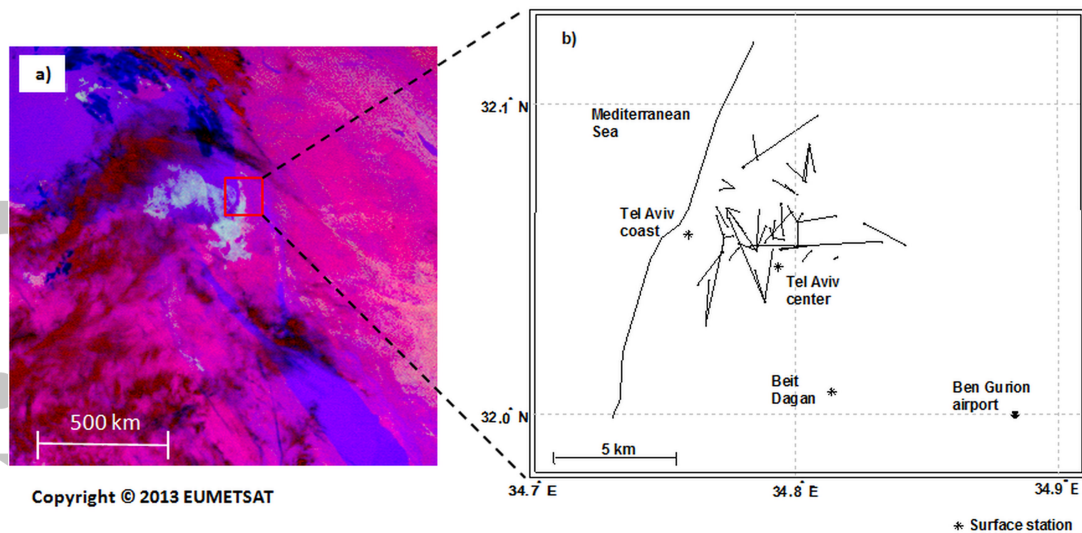


**Figure 3.** The observed area. **(a)** The image was taken by Meteosat Second Generation (MSG) at 01:27 on 10 December 2005. The wide fog front (tens of km in scale) is indicated in the image in white. The square (red) indicates the area we focused on in our research. **(b)** Map of the MLs and measurement instruments in the observed area. The 88 MLs at the site are deployed over 47 physical paths and span an area of  $5 \times 6 \text{ km}^2$ . Three transmissometers, and a professional human observer are located at Ben Gurion airport (41 m ASL). The three meteorological ground stations (5-35 m ASL) are indicated by asterisks. An additional human observer is located at the Beit Dagan ground station (35 m ASL).

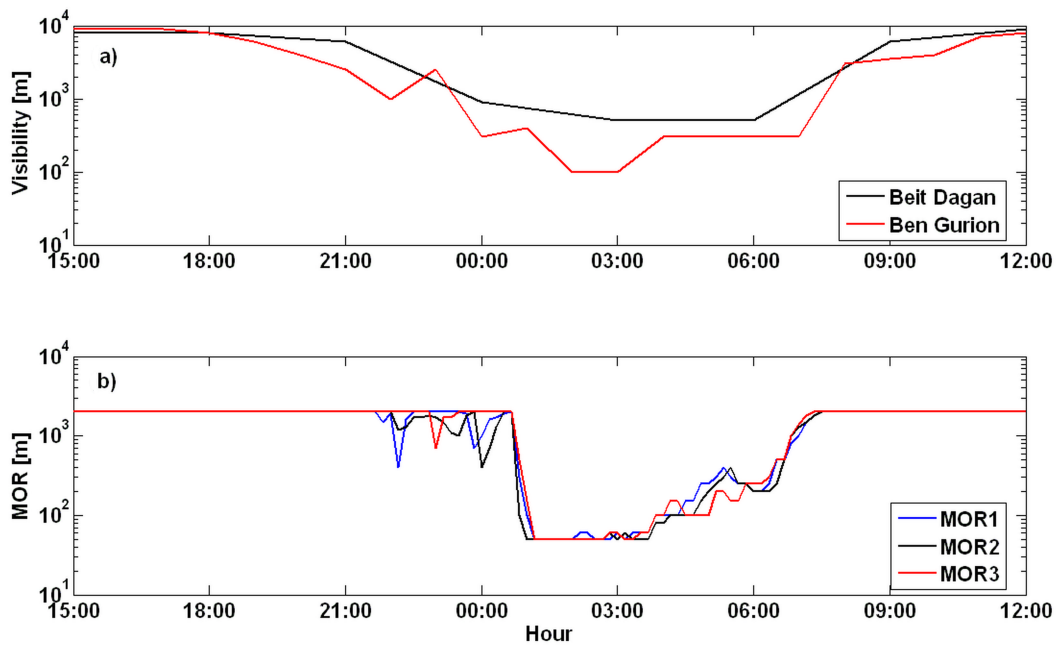


**Figure 4.** Visibility assessments. The assessments were carried out between the hours of 15:00 on 9 December, and 12:00 on 10 December, 2005, respectively. (a). Visibility assessments as registered by the human observer at the Beit Dagan meteorological station and Ben Gurion airport. Assessments were made once every 3 hours by the observer located at Beit Dagan and once an hour by the Ben Gurion observer. Fog was detected between 00:00 to 06:00- 07:00. (b). MOR measurements taken by three transmissometers located at Ben Gurion airport. The instruments are arrayed over three separate 50 m visual paths at an elevation of 2.5m AGL (The figure is based on instantaneous measurements at 10 minute intervals). According to these instruments, fog was detected starting from around 22:00 till 07:00 of the following morning.

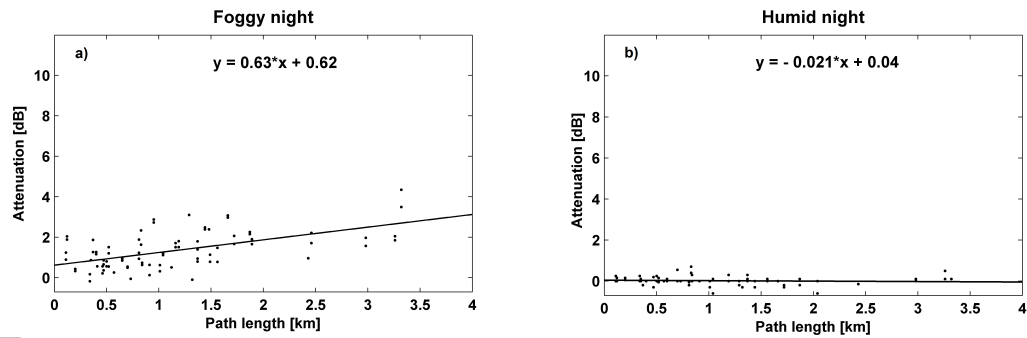


**Figure 5:** Microwave attenuation measurements. The attenuation measurements, as measured by the MLs system on a foggy (10 December) night **(a)** and during a humid night (15 December) without fog **(b)**. Every point represents a measurement from a single link, taken around 01:30. The linear fit approximations of the measurement sets are listed at the top of each panel. The slope of the graph in (a) represents the effective attenuation measured in the fog patch (based on 88 microwave samples), where the y-axis intercept represents the estimated attenuation as a result of antenna wetness. The slope of the graph generated for the non foggy night, as well as the y-intercept tend to zero (based on 68 samples acquired according to the availability of RSL data from the system during that night).

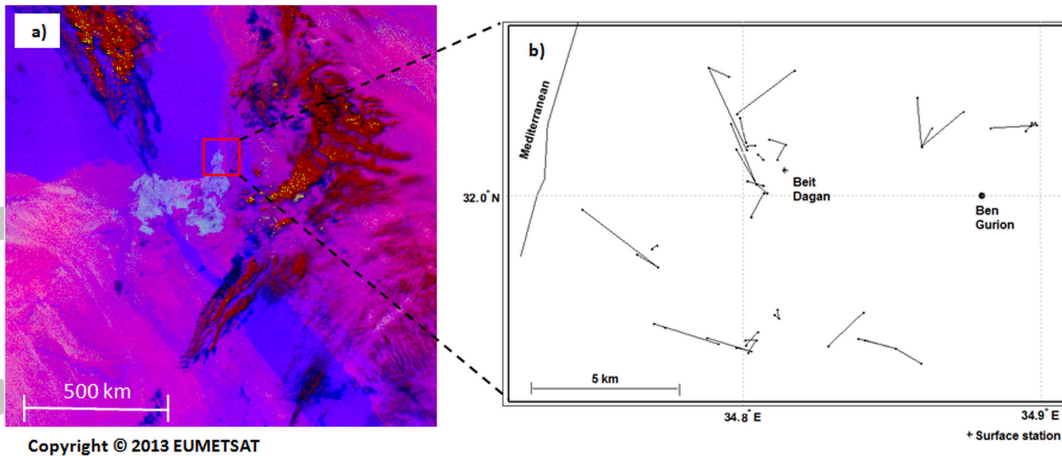


**Figure 6.** The observed area. **(a)**. The image was taken by the MSG satellite on 16 November 2010, 00:34 h. The fog is indicated in white and the study area by the red-square. **(b)**. Map of the MLs and measurement instruments in the observed area. The 58 MLs in the area are deployed over 39 physical paths and spread across an area of about  $15 \times 10$  km. Measurements are obtained once every 24 hours at 22:00 (satellite Images which were acquired around this hour during the event did not provide clear indication for the fog in the region due to middle and high altitude cloud cover that obstructed the satellite line of sight to the ground). There are three transmissometers located at Ben Gurion airport (41m ASL) as well as a human observer. Another human observer, as well as a scattermeter are located at the Beit Dagan ground station (35m ASL).

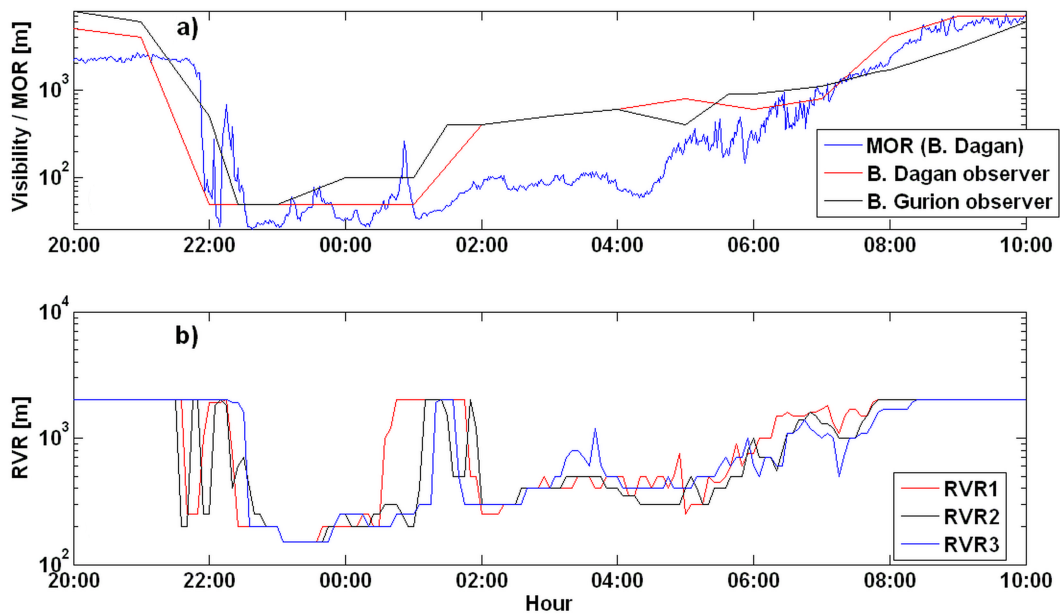


**Figure 7.** Visibility and RVR measurements. The observations were taken between November 15 and November 16, 2010, between 20:00 and 10:00 the following day. **(a)**. Visibility assessments as registered by the human observers (at the Ben Gurion and Beit Dagan station). Observations were taken once an hour by each observer (the Beit Dagan observer estimates between 22:00 to 01:00 of several meters to 100 m, were plotted as 50 m during this time frame). Also depicted are MOR measurements at 1 minute intervals which were acquired by a scattermeter located in Beit Dagan. **(b)**. RVR measurements taken by the three transmissometers deployed at the airport over three different physical paths (the plot is based on instantaneous measurements at 5 minute intervals.).

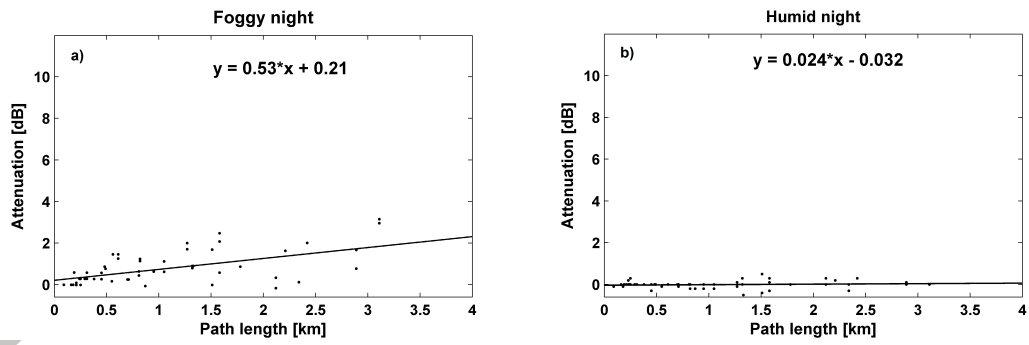


**Figure 8.** Microwave system measurements. Observations taken on the foggy night, 15 November 2010 **(a)**, and those taken on the humid night, 10 November 2010 **(b)**. Each point represents a measurement from a single link, taken simultaneously at 22:00. The linear fit approximations of the measurement sets for each night are listed at the top of each panel.

Accepted Article